JACS
JOURNAL OF THE AMERICAN CHEMICAL SOCIETY
Article
pubs.acs.org/JACS

First-Principles Prediction of Thermodynamically Stable Two-Dimensional Electrides

Wenmei Ming,[†,‡] Mina Yoon,*[,†,§] Mao-Hua Du,[‡] Kimoon Lee,[∥] and Sung Wng Kim*[,⊥]

[†]Center for Nanophase Materials Sciences, Oak Ridge National Laboratory, Oak Ridge, Tennessee 37831, United States
[‡]Materials Science & Technology Division, Oak Ridge National Laboratory, Oak Ridge, Tennessee 37831, United States
[§]Department of Physics and Astronomy, University of Tennessee, Knoxville, Tennessee 37916, United States
[∥]Department of Physics, Kunsan National University, 558 Daehak-ro, Gunsan, Jeonbuk 573-701, South Korea
[⊥]Department of Energy Science, Sungkyunkwan University, 300 Cheoncheon-dong, Jangan-gu, Suwon, Gyeonggi-do 440-746, South Korea

Supporting Information

ABSTRACT: Two-dimensional (2D) electrides, emerging as a new type of layered material whose electrons are confined in interlayer spaces instead of at atomic proximities, are receiving interest for their high performance in various (opto)electronics and catalytic applications. Experimentally, however, 2D electrides have been only found in a couple of layered nitrides and carbides. Here, we report new thermodynamically stable alkaline-earth based 2D electrides by using a first-principles global structure optimization method, phonon spectrum analysis, and molecular dynamics simulation. The method was applied to binary compounds consisting of alkaline-earth elements as cations and group VA, VIA, or VIIA nonmetal elements as anions. We revealed that the stability of a layered 2D electride structure is closely related to the cation/anion size ratio; stable 2D electrides possess a sufficiently large cation/anion size ratio to minimize electrostatic energy among cations, anions, and anionic electrons. Our work demonstrates a new avenue to the discovery of thermodynamically stable 2D electrides beyond experimental material databases and provides new insight into the principles of electride design.

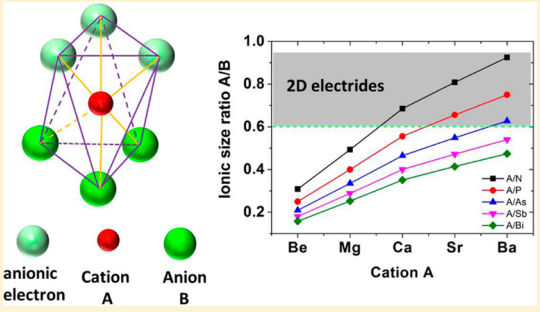

INTRODUCTION

An electride[1,2] is a unique type of ionic compounds, where the electrons mostly distribute in the structural cavities of a lattice, behaving as anions. Such electron distribution is significantly different from the conventional picture in covalent and ionic compounds, where electrons are distributed to form bonds between atoms. Because of the less tightly bound nature of the interstitial electrons in the cavities than around the atoms, electrides can possess a high degree of mobility[3] and a low work function,[4] which makes them promising in applications such as highly conducting electrodes,[3] efficient thermionic emitters,[5] low injection-barrier cathodes[6,7] for organic light-emitting diodes, and high performance catalysts.[8−11]

Organic electrides, such as organic salts of alkali metal,[12,13] synthesized in the early stage of electride materials development, were not stable at room temperature and ambient condition. More recently synthesized inorganic electrides, on the other hand, have significantly improved their thermal and chemical stability. Specifically, the discovery of inorganic electrides with a significantly higher thermal and chemical stability at room temperature[4,5] have opened a new era in electride materials research and application. However, synthesis of a stable electride is still a grand challenge in the field, and only a few inorganic electrides have been successfully synthesized during the past decade. The synthesized materials include three-dimensional (3D) $Ca_{24}Al_{28}O_{64}{:}4e^-$ [3] and layered $Ca_2N{:}e^-$,[14] where the former has interstitial electrons occupying the cages of the six Ca coordinated framework and the latter has interstitial electrons occupying the two-dimensional (2D) interlayer spaces sandwiched by Ca−N−Ca trilayers (thus the name "2D electride"). By assuming all ions take their formal oxidation numbers, both of them have excess unsaturated electrons ($4e^-$ and $1e^-$ in the chemical formula of $[Ca_{24}Al_{28}O_{64}]^{4+}{\cdot}4e^-$ and $[Ca_2N]^+{\cdot}e^-$, respectively), which turns out to be the reason for making them metallic instead of otherwise insulating when the electrons are fully saturated.[15,16]

Structurally, it is interesting to notice that $Ca_{24}Al_{28}O_{64}$ was synthesized from its electron saturated counterpart $Ca_{24}Al_{28}O_{66}$ by selectively removing two oxygens per formula unit from the cage centers through oxygen-reducing processes in the experiment,[3] leaving behind two vacant oxygen sites into which four excess electrons could fit. Similarly, Ca_2N can be viewed to form from the experimentally existing layered ionic compound Ca_2NX (X = Cl, Br, or I)[17,18] by removing X, which may be seen as the intercalation layer of Ca_2N; hence the

Received: June 7, 2016
Published: October 21, 2016

DOI: 10.1021/jacs.6b05586
J. Am. Chem. Soc. 2016, 138, 15336−15344

resulting vacant X sites will serve as electron sinks for the excess electrons. The same mechanism also applies to the most recently discovered one-dimensional electride $La_8Sr_2(SiO_4)_6$, synthesized by partially removing oxygens from electron-saturated $La_8Sr_2(SiO_4)_6O_2$ precursor.[19] Therefore, it is plausible to deem an electride as a derivative of its electron-saturated counterpart, with stoichiometric anion deficiency.

This physical picture of an electride is similar to that of the well-known F-center in alkaline halides.[20] As a halogen vacancy defect, the F-center has a very low concentration in comparison to the number of available halogen sites. Electrides, on the other hand, contain a stoichiometric concentration of anion vacancy but at the same time still remains stable without metallization (i.e., direct cation−cation bonding), where each anion vacancy is surrounded by cation nearest neighbors, thus offering a new type of electronic structure in terms of stoichiometric deficiency of associated anions.

Together with the recent surge of interest in 2D materials, due to the capability of making devices as small as a few atomic layers in thicknesses, is an increasing effort in searching for new 2D electrides. High-throughput ab initio screening[21,22] based on available materials databases has been employed to discover possible 2D electrides. Only very few candidates of alkaline-earth nitrides (Ca_2N, Sr_2N, and Ba_2N) and transition-metal/rare-earth carbides (Y_2C, Tb_2C, Dy_2C, and Ho_2C) have been found. Although density functional theory (DFT) calculations have shown that only the alkaline-earth nitrides have interstitial electrons mainly confined within cation interlayer space, transition-metal/rare-earth carbides have a significantly smaller electron distribution within the cation interlayer space due to significant charge occupation within the cationic layers,[22] making them less attractive as electrides. The previous theoretical effort[21,22] was restricted into materials only available in experimental material databases, hence it significantly limits the search space. On the basis of the search results, the paper[21] further proposes a few layered crystal structures as potential electrides. However, they were manually constructed, instead of by using thorough structure search algorithms and structure optimization, that is, they are hypothetical. A recent study[23] employs global structure search to identify electrides by optimizing electron localization function instead of globally minimizing total energy. Therefore, the predicted structures are not necessarily energetically favorable among the populated structures in the search space. Specifically, their thermodynamic stability was unexplored, thus it is not clear at all whether they equate to real material. Additionally, no study so far has identified any design rules for electrides that go beyond the simple oxidation counting and count on their structure stability.

We are therefore motivated to use a different and theoretically more satisfactory approach to predicting new 2D electride candidates that are experimentally accessible. Our approach combines the global structure optimization method[24] and DFT calculations for total energy, phonon spectrum, and molecular dynamics, which enables us to find thermodynamically stable ground state structure of a crystalline material with only an input of chemical composition. We have applied the approach to simple systems of A_2B (where A and B are cations and anions, for each, A/B = alkaline-earth elements/group VA or VIA nonmetal elements) and AB (A/B = alkaline-earth elements/halogens), which all have imbalanced nominal oxidation numbers. We have found several new 2D electrides, which are hexagonal crystals for A_2B and tetragonal crystals for AB. Most importantly, we have revealed the important design rule of cation/anion size ratio in effecting the successful formation of 2D electrides.

CALCULATION DETAILS

Our structural predictions are based on the global structure search method with the particle swarm optimization (PSO) algorithm implemented in the Calypso code.[25] The structures generated by Calypso at each generation are then optimized to local minima and subsequently the total energy energies are calculated by using the DFT VASP code.[26] For structure prediction calculations performed using the Calypso code, we use simulation cells containing from one to four chemical formula units of each binary compound ever tried. The number of structures in each generation is 24 and the total number of generations is 25 during the structure evolution. Because randomly generated structures (40% of the total number of structures) are included in each generation (in the very first generation, all structures are randomly generated), each prediction for the electrides was repeated four times to make sure the same ground state structures can always appear in the final generation. For VASP calculations, we employ the projector augment wave type pseudopotential[27] and the Perdew−Burke−Ernzerhof (PBE) version of the exchange-correlation functional.[28] A 520 eV kinetic energy cutoff and Γ-centered *k*-mesh with *k*-spacing of 0.4/Å are used for structure relaxation and a denser *k*-mesh with *k*-spacing of 0.15/Å for total energy calculation. During structure relaxation, both lattice constants and atom coordinates are optimized until the force at each atom is smaller than 0.02 eV/Å. We note that even though 2D electrides have large interlayer distance greater than 3 Å, PBE functional without van der Waals (vdW) correction is sufficient to obtain a reliable structure, because anionic interstitial electrons exist in the interlayer space, making the interlayer electrostatic interaction much stronger than a typical vdW interaction commonly encountered in layered covalent materials.

An apparent condition for the formation of electride is that the sum of the common oxidation numbers of all the constituent ions should be positive, so that overall charge neutrality requires excess electrons, which may prefer to stay in the void regions of a lattice. Our chosen compositions A_2B (A/B = alkaline-earth elements/group VA, VIA nonmetal elements) and AB (A/B = alkaline-earth elements/halogens) both satisfy this condition. As we learn from the experimentally confirmed 2D electrides (Ca_2N[14] and Y_2C[29]), excess electrons are sandwiched by positive cation layers and thus are stabilized by the attractive electrostatic interaction between the negative anionic electrons and the positive cation layers. We hence identify 2D electride candidates from those whose predicted ground-state structures have cation sandwiched interlayer spaces and particularly contain no direct metal−metal bonding, which will give rise to the appearance of conventional electron distribution as seen in metallic bonds. Specifically, our study concerns the stoichiometric compositions of A_2B and AB with possible stacking sequences of interlayer spaces [see Figure 1a for A_2B and in Figure 1b1,b2 for AB]. In A_2B, A is alkaline-earth metal and B is VA or VIA nonmetal. In AB, A is alkaline-earth metal and B is a halogen element.

RESULTS AND DISCUSSION

We first focus on the ground-state structure prediction of A_2B with A from alkaline-earth elements and B from VA elements, where the sum of all the oxidation numbers is +1. Because of the chemical similarity of the constituent elements, A_2B's are expected to have a structure similar to that of Ca_2N if they can assume a layered configuration. As a benchmark, we first confirmed that our lowest energy structures of Ca_2N, Sr_2N, and Ba_2N are consistent with those in the ICSD materials database.[22] Table 1 summarizes our A_2B and AB results. The bold and italic indicate that the predicted ground state has a 2D layered structure with cation sandwiched interlayer spaces as described in the last paragraph. Therefore, it can be a 2D electride and has further been verified by electronic structure

DOI: 10.1021/jacs.6b05586
J. Am. Chem. Soc. 2016, 138, 15336−15344

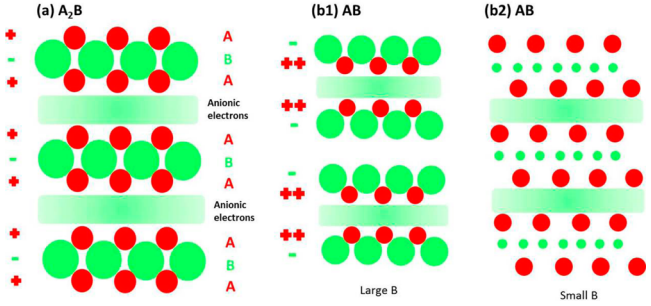

Figure 1. Schematics of ion stacking sequences to form cation sandwiched interlayer spaces, (a) for stoichiometry A_2B where representative +1 (+) and −1 (−) ionic charges are assigned to A and B, respectively; (b) for stoichiometry AB where representative +2 (++) and −1 (−) ionic charges are assigned to A and B, respectively. When anion B is significantly larger than cation A, the sequence may assume b1. When anion B is smaller than anion A, the sequence may assume b2, where the B anionic layers are inserted in-between A layers.

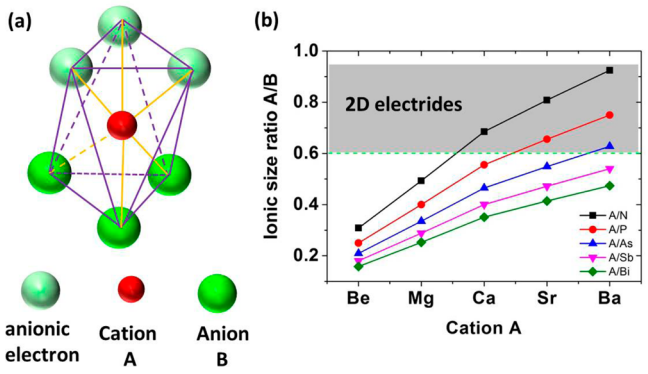

Figure 2. (a) Schematic octahedron in Ca_2N, composed of cation A(Ca), anion B(N), and anionic electron. (b) Ionic size ratio of A to B as a function of different cation A. The dark gray shaded area denotes the chemical region of A_2B, which can have layered structure in its ground state from the structure prediction. See Table S2 in the Supporting Information for the ionic sizes used.

calculation in a later section of this paper that it is indeed a 2D electride. Note that the bold ones are newly identified 2D electrides by this study. The otherwise indicates that the predicted ground state does not have such desired 2D layered structure and cannot be 2D electride, thus no further electronic structure calculation has been conducted in such situation. We identified three new electrides with 2D layered structures as ground states. They are Sr_2P, Ba_2P, and Ba_2As, for A_2B, which share the same crystal space group ($R\bar{3}m$, #166) as Ca_2N. The structure similarity between them may be due to the chemical similarity among Ca/Sr/Ba and N/P/As. On the other hand, it is interesting to note that early alkaline-earth nitrides, such as Be_2N and Mg_2N, do not have a 2D layered ground-state structure, whereas the nitrides A_2N (A = Ca, Sr, and Ba) are well-established 2D electrides. Generally, A_2B stabilizes against layered structures as size of B increases, as indicated in Table 1, in that their structural stability has a strong dependence on the size ratio of anion B to cation A.

The size ratio dependence becomes mandatory if we take electride electrons as equivalent anionic species that have predefined crystalline sites on which to sit[30−32] (hereafter, we term electride electron as anionic electron). Using an ionic polyhedron model similar to that used in deriving Pauling's rules,[33] where anions occupy the polyhedron corners and a cation occupies the center coordinating with the anions, we could assign anion B's and anionic electrons at the corners of the polyhedron and cation A at the center. For A_2B with the structure of Ca_2N, the polyhedron is an octahedron as sketched in Figure 2a. The stability is roughly determined by two opposite electrostatic energies: attractive energy between cation A and anion B's/anionic electrons and repulsive energy between anions (B's and anionic electrons). So with respect to B, A should be sufficiently large to avoid overlapping between the anions; at the same time, A should not be too large to retain its coordination number with B (polyhedron). This argument well explains Figure 2b presenting stable 2D electrides in ionic size ratio. The predicted layered electrides of A_2B from Table 1 all sit in the dark gray shaded region, where the ionic size ratio of cation A/anion B is greater than ∼0.6, and all other non-2D electrides of smaller ionic size ratio lie below that region.

We further investigated possible A_2B electrides consisting of chalcogenide anions (group VIA, O, S, Se, and Te) and alkaline-earth metal cations. However, we were not able to identify any 2D layered ground-state structures as electrides in this category (see Table 1). In terms of ionic size, the VIA anion (2e charge) is smaller than its corresponding (same row) VA anion (3e charge), so at a given A the size ratio of A/B is larger with B of VIA anion than that with B of VA anion, which seemingly indicates that more layered structures should be favored in A_2B (B = VIA). However, A_2B (B = VIA) (2e) has more anionic electrons than A_2B (VA) (1e), which gives a larger-sized anionic electron and causes stronger Coulombic repulsion between anionic electrons if it still assumes a layered structure. Therefore, layered electrides are absent in A_2B with B = VIA. Additionally, we point out that in general for A_2B, the more excess electrons A has with respect to the nominal oxidation number of B, the less tendency A and B have to remain ionic to form electride. For example, Ca_2N has only 0.5-excess-electron/Ca, where all the Ca forms direct ionic bonds with N. Instead, Ca_2O has 1-excess-electron/Ca, where part of the Ca forms metal layers with direct Ca−Ca bonds (see

Table 1. Determination of the Existence of 2D Layered Electrides in Predicated Ground State Structure A_2B and AB[a]

	group VA					group VIA				group VIIA			
	N	P	As	Sb	Bi	O	S	Se	Te	F	Cl	Br	I
Be	Be_2N	Be_2P	Be_2As	Be_2Sb	Be_2Bi	Be_2O	Be_2S	Be_2Se	Be_2Te	BeF	BeCl	BeBr	BeI
Mg	Mg_2N	Mg_2P	Mg_2As	Mg_2Sb	Mg_2Bi	Mg_2O	Mg_2S	Mg_2Se	Mg_2Te	MgF	MgCl	MgBr	MgI
Ca	*Ca_2N*	Ca_2P	Ca_2As	Ca_2Sb	Ca_2Bi	Ca_2O	Ca_2S	Ca_2Se	Ca_2Te	**CaF**	CaCl	CaBr	CaI
Sr	*Sr_2N*	**Sr_2P**	Sr_2As	Sr_2Sb	Sr_2Bi	Sr_2O	Sr_2S	Sr_2Se	Sr_2Te	**SrF**	SrCl	SrBr	SrI
Ba	*Ba_2N*	**Ba_2P**	**Ba_2As**	Ba_2Sb	Ba_2Bi	Ba_2O	Ba_2S	Ba_2Se	Ba_2Te	**BaF**	BaCl	BaBr	BaI

[a]Bold and italic indicate the existence of 2D electrides. Bold ones are newly identified 2D electrides by this study.

DOI: 10.1021/jacs.6b05586
J. Am. Chem. Soc. 2016, 138, 15336−15344

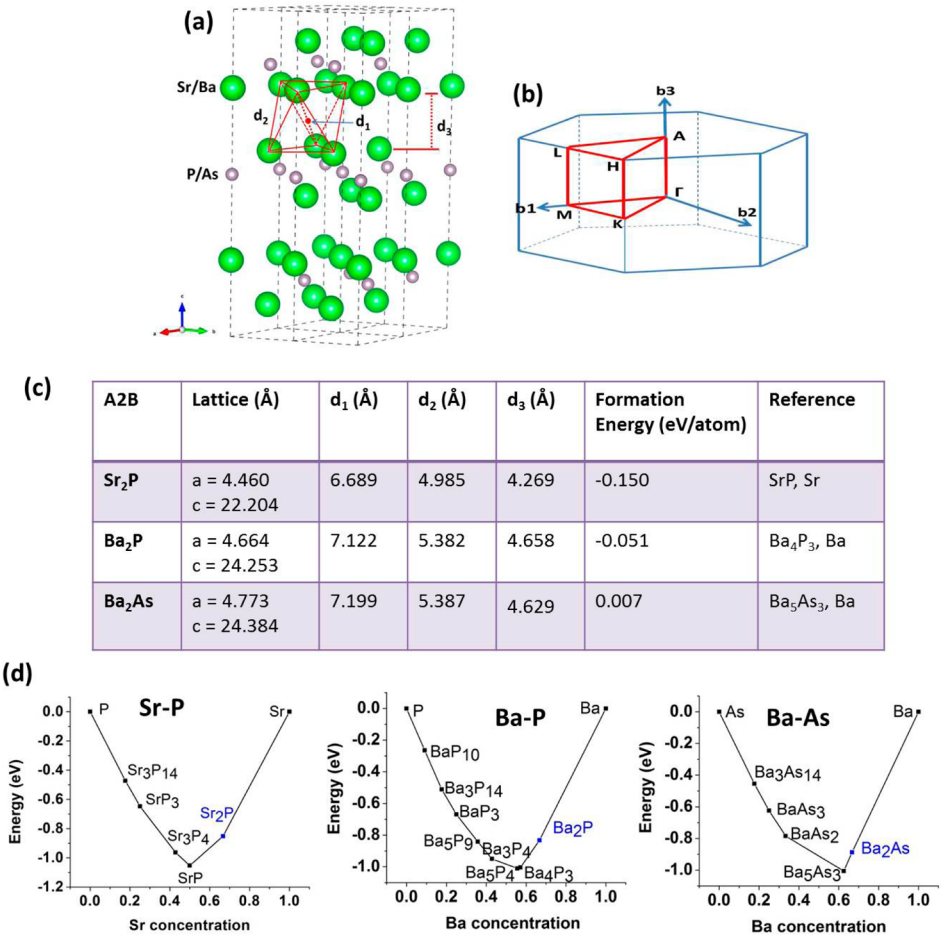

(c)

A2B	Lattice (Å)	d_1 (Å)	d_2 (Å)	d_3 (Å)	Formation Energy (eV/atom)	Reference
Sr_2P	a = 4.460 c = 22.204	6.689	4.985	4.269	-0.150	SrP, Sr
Ba_2P	a = 4.664 c = 24.253	7.122	5.382	4.658	-0.051	Ba_4P_3, Ba
Ba_2As	a = 4.773 c = 24.384	7.199	5.387	4.629	0.007	Ba_5As_3, Ba

Figure 3. Crystal structure information and formation energy of the three new layered A_2B (Sr_2P, Ba_2P, and Ba_2As): (a) The figure at left illustrates their hexagonal crystal structure with space group $R\bar{3}m$ (#166). d_1 is the distance between the two axial metal cations from adjacent two cation interlayers. The red dot illustrates the center where anionic electron is expected to site. d_2 is the distance between the nearest metal cation−cation from adjacent two cation interlayers. d_3 is the vertical distance between two adjacent cation interlayers. (b) The corresponding Brillouin zone and high symmetry *k*-point path. (c) Basic structure information and formation energies for the three 2D electrides (Sr_2P, Ba_2P, and Ba_2As). The reference column in the table gives the stable reference materials in crystalline bulk for the formation energy calculation of A_2B. The material choice is made via the corresponding convex hulls of phase diagrams (in panel d), where the two material references with closest composition to the electride under study are chosen. (d) The convex hulls were reproduced using the DFT calculated energies data (in black color) for only experimentally already existing compositions for each binary system (left, Sr−P; middle, Ba−P; right, Ba−As) from Materials Project Database.[36] We also added our predicted electrides (in blue color) into the convex hulls.

Supporting Information Figure S1). A limiting scenario is that A_nB ($n \rightarrow \infty$), which is essentially a metal, has 2-excess-electrons/A if A and B still take their ionic oxidation numbers. These excess electrons, however, have no void spaces and thus form metallic bonds. Similar gradual metallization with increasing excess electrons has also been observed in nonstoichiometric ionic clusters.[34,35]

We now focus on analyzing the basic properties of the newly identified A_2B electrides, Sr_2P, Ba_2P, and Ba_2As. Information on their crystal structures (see more details in Supporting Information Table S1) and formation energies is given in Figure 3. They all have the same hexagonal crystal structure with space group $R\bar{3}m$ (#166) as Ca_2N. In comparison with experimentally existing stable crystalline compounds A_xB_y, the predicted 2D electrides contain the highest concentration of cations (A) (Figure 3d). Therefore, the additional cations (A) supplied in the reaction with A_xB_y are necessary to obtain the A-rich 2D electrides predicted in this study, where reference materials for the formation of the electride should be a stable A_xB_y compound and elemental A with the formation energy of electrides as ΔH_f(electride): $\Delta H_f(\text{electride}) = [E(\text{electride } A_{x+1}B_y) - E(A_xB_y) - E(A)]/(x + 1 + y)$, where E is the energy per formula unit of the material indicated in parentheses. Figure 3d shows convex hull phase diagrams for Sr−P (left panel), Ba−P (middle panel), and Ba−As (right panel), which can be used to determine uniquely the energetic stability of a material against spinodal decomposition in thermodynamics. All the chemical formulas except the electrides (colored in blue) correspond to experimentally existing stable crystalline materials in the Materials Project Database[36] or ICSD Database.[22] The chemical formulas in blue indicate the 2D electrides predicted from our work. From the convex hull, we took A_xB_y, which in stoichiometry is closest to our 2D electride and the corresponding elemental A (Sr, Ba) as the reference material, which are the only required references to uniquely determine the thermodynamic stability of our electrides. For better visualization of the energetic stability, we have added the predicted electrides (blue dots) onto the convex hull lines. Figure 3c presents the formation energies of Sr_2P and Ba_2P are negative with respect to existing stable reference materials,

DOI: 10.1021/jacs.6b05586
J. Am. Chem. Soc. 2016, 138, 15336−15344

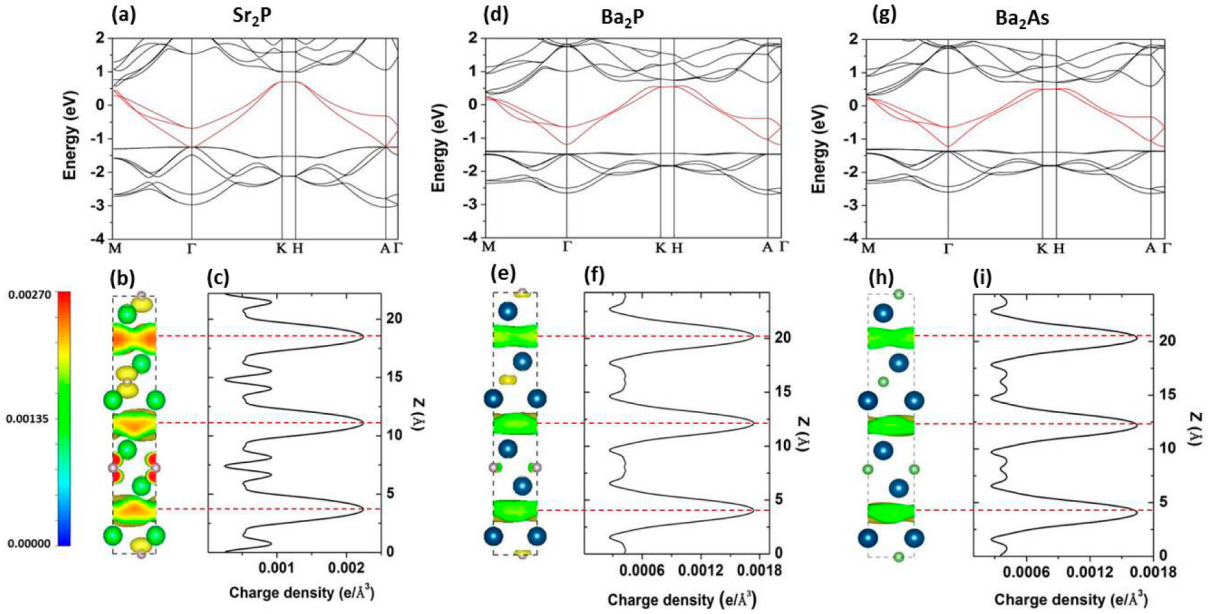

Figure 4. Electronic structures of thermodynamically stable electrides. Band structures of Sr_2P (a), Ba_2P(d), and Ba_2As (g). Isosurfaces (1.35×10^{-3} e/Å^3) of partial charge density $n(r)$ of states within 0.1 eV below Fermi energy for Sr_2P(b), Ba_2P(e), and Ba_2As (h), with planar averaged charge density along z (c,f,i).

indicating the possibility of synthesizing them from the reference materials. Ba_2As has very small positive formation energy (7 meV/atom), signifying it may be synthesizable too.

We confirm that Sr and Ba atoms in the predicted 2D electrides form pure ionic bonding. The nearest metal−metal (M−M) interatomic distance (d_2) is 4.985, 5.382, and 5.387 Å for Sr_2P, Ba_2P, and Ba_2As, respectively, as presented in Figure 3c. In comparison, the nearest interatomic distance for elemental Sr and Ba metals (FCC and BCC structures, respectively, at room temperature) is 4.296 and 4.339 Å, for each. Thus, the interatomic M−M distances of our predicted electrides are all at least 0.7 Å greater than that in the elemental metals M, which excludes the possibility of direct M−M bonding. Furthermore, within each trilayer of Sr−P−Sr, Ba−P−Ba, and Ba−As−Ba of our predicted electrides, the bond lengths of Sr−P, Ba−P, and Ba−As are extremely close to the sum of the respective ionic radii, considering the bond lengths: another indication supporting their ionic bonding characteristic. The bond lengths are Sr−P = 3.014 Å, Ba−P = 3.192 Å, and Ba−As = 3.265 Å, and the typical ionic radii R are $R(Sr^{2+})$ = 1.18 Å, $R(Ba^{2+})$ = 1.35 Å, $R(P^{3-})$ = 1.80 Å, and $R(As^{3-})$ = 2.15 Å, which give $R(Sr^{2+}) + R(P^{3-})$ = 2.98, $R(Ba^{2+}) + R(P^{3-})$ = 3.15, and $R(Ba^{2+}) + R(As^{3-})$ = 3.50 Å. Similarly, in the predicted CaF, SrF, and BaF, the bond lengths of Ca−F, Sr−F, and Ba−F are 2.354, 2.523, and 2.626 Å. The typical ionic radii R are $R(Ca^{2+})$ = 1.00, $R(Sr^{2+})$ = 1.18 Å, $R(Ba^{2+})$ = 1.35 Å, and $R(F^-)$ = 1.33. Thus, the sums of ionic radii are $R(Ca^{2+}) + R(F^-)$ = 2.33 Å, $R(Sr^{2+}) + R(F^-)$ = 2.51 Å, and $R(Ba^{2+}) + R(F^-)$ = 2.68 Å, which are very close to the respective bond lengths of Ca−F, Sr−F, and Ba−F, respectively. It supports that Ca, Sr, and Ba form ionic bonds in the predicted CaF, SrF, and BaF. At the same time, the nearest interlayer M−M distances are 4.165, 4.540, and 5.199 Å. Therefore, we postulate that in our predicted electrides, M (Ca, Sr, Ba) should be legitimately taken as a normal ion rather than as a simple metal atom as seen in elemental metal. The large interlayer M−M interatomic distance excludes the possibility of direct M−M bonding. On the basis of this ionic picture for Ca, Sr, and Ba in our predicted electrides, the interlayer space expected to accommodate electride electrons (anionic electrons) then will become significantly larger than that for pure metals, as an electride has dramatically smaller ionic size than the counterpart atomic size in pure metal. We thus conclude that the anionic electrons are not related to M−M bonding.

Additionally, we calculate the electron localization functions (ELFs) of the predicted electrides, Sr_2P, Ba_2P, Ba_2As, CaF, SrF, and BaF (see Supporting Information Figure S2). ELF evaluates the degree of spatial localization of electrons.[15] In agreement with our bond length arguments above, ELFs show clearly that Sr and Ba are ionic characteristic in all the predicted electrides.

Next, we studied the electronic structures of the new electrides. Figure 4a,d,g exhibits their electronic band structures, which are very similar in band dispersion owing to their chemical and structural similarities. We highlight the bands whose corresponding charge density is mainly distributed in the interlayer spaces in red, where the bandwidth (defined as difference between energies at M and Γ) decreases by 0.25 eV from 2.00 eV in Sr_2P to 1.75 eV in Ba_2P and Ba_2As because of the increase in lattice constant. The partial electron density, $n(r) = \int_{E_f - 0.1}^{E_f} |\varphi(r, E)|^2 dE$, is plotted in Figure 4b,e,h with isosurface value of 1.35×10^{-3} e/Å^3, where a substantial portion of charges are localized in the interlayer space between cations. The localization feature can be further quantified by planar averaged charge density along the z direction, $n(z) = \frac{1}{A}\int n(r)dxdy$, where A is the unit cell area in xy-plane (see Figure 4c,f,i). Charge density peaks occur at the middle plane of the interlayer spaces with the significantly lower tails extending into the ionic layers, which clearly supports the typical characteristics of 2D electride for our predicted structures.

We evaluated the amount of anionic electrons near the Fermi level E_f (i.e., the portion of charges confined in the 2D

DOI: 10.1021/jacs.6b05586
J. Am. Chem. Soc. 2016, 138, 15336−15344

interlayer space among the total charges). Previously, it was defined as[21]

$$P'_{\text{ani}} = \frac{\int_{V_{\text{emp}}} \mathrm{d}r \int_{E_f-\Delta E}^{E_f+\Delta E} n(r, E)\mathrm{d}E}{\int_{V} \mathrm{d}r \int_{E_f-\Delta E}^{E_f+\Delta E} n(r, E)\mathrm{d}E} \quad (1)$$

where V is the unit cell volume, V_{emp} is the volume of anionic electrons residing in interlayer space, and ΔE is the size of the energy interval centered at the Fermi energy E_f (ΔE of 0.1 eV is used). Here, V_{emp} is approximated by the unit cell volume minus the volumes of ionic spheres, which includes the interstitial volumes between ions, thus resulting in an upper limit value of anionic electron localization percentage. Our definition that further excludes the interstitial volumes is

$$P_{\text{ani}} = \frac{\iint_{A} \mathrm{d}x\mathrm{d}y \int_{z'} \mathrm{d}z \int_{E_f-\Delta E}^{E_f+\Delta E} n(r, E)\mathrm{d}E}{\int_{V} \mathrm{d}r \int_{E_f-\Delta E}^{E_f+\Delta E} n(r, E)\mathrm{d}E} \quad (2)$$

where z' coordinate is only in interlayer space, so we can obtain the ratio of anionic electron purely inside interlayer space, delineating a lower limit value. The calculated P_{ani} and P'_{ani} values based on the two definitions, eqs 1 and 2, respectively, are compared in Figure 5. Depending on the definition, the

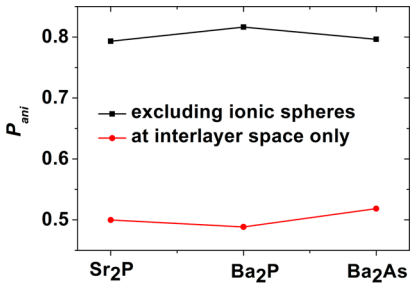

Figure 5. Anionic electron ratio P_{ani} calculated under the two definitions with different volumes for anion electrons: "exluding ionic spheres" has interlayer spaces and interstitial volumes, whereas "at interlayer space only" has interlayer spaces only. See the main text for details.

values lie in a large range but the conclusion is clear: for the three predicted A_2B's, a significant amount of charges (>50%) near the Fermi level are located in interlayer space.

Because of the interlayer electron distribution, Sr_2P, Ba_2P, and Ba_2As are expected to have low work function. We calculated their work functions on surfaces (0001) and (11$\bar{2}$0); the (0001) surface is cleaved parallel through interlayer space, and the (11$\bar{2}$0) surface is cleaved perpendicular through ionic layers (see Figure 6a) (see details of work function calculations in Supporting Information Figures S3–S9). As presented in Figure 6b, first, the work functions exhibit large surface anisotropy with a lower value on (11$\bar{2}$0) than on (0001); second, the work function of surface (0001) monotonically decreases from 2.8 to 2.58 eV from Sr_2P to Ba_2As; third, the work function of surface (11$\bar{2}$0) has the lowest of ~2.1 eV at Ba_2P. It is well-known that surface anisotropy of work function in transition metals originates from Smoluchowski smoothing[37,38] (surface charge smoothing), which creates a larger positive surface dipole on a surface with corrugated charge distribution than on a surface with smooth charge distribution, hence giving a charge corrugated surface a lower vacuum level

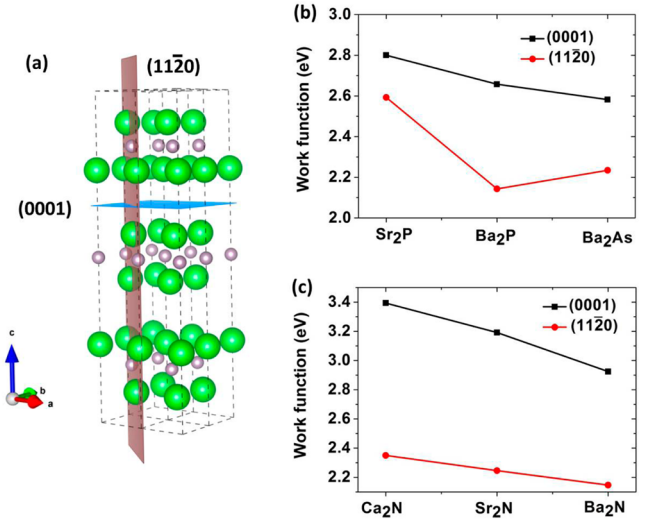

Figure 6. (a) Schematics of lattice planes (0001) and (11$\bar{2}$0). (b) Work functions of Sr_2P, Ba_2P, and Ba_2As at surface (0001) and (11$\bar{2}$0). (c) For comparison, work function of Ca_2N, Sr_2N, and Ba_2N are also shown.

and lower work function. According to this picture, work function (W) can be written as

$$W = (E_{\text{vacc}} - \Delta E_{\text{dipole}}) - E_f \quad (3)$$

where E_{vacc} is the vacuum level (when assuming surface charge distribution is the same as bulk) and ΔE_{dipole} is the reduction of vacuum level from surface charge smoothing. Because the (0001) surface with nucleus-free electride electron charge is significantly smoother than the bond cutting surface (11$\bar{2}$0), it has much less surface charge smoothing ΔE_{dipole} and thus higher work function. Also, we note that the attractive electrostatic potential at the anionic electron site decreases with increasing distance d (=0.5d_1) (see Figure 3c for d_1 values) between cation and anionic electron site from Sr_2P to Ba_2As, and the Fermi energy E_f should increase accordingly; therefore, we see the monotonic decrease of work function in the second trend. Furthermore, the combined effects of the variations of both ΔE_{dipole} and E_f should be taken into account for surface (11$\bar{2}$0). Particularly, because Ba–P exhibits more characteristics of ionic bonding than does Ba–As due to the larger electronegativity of P than As, we expect a more corrugated surface (11$\bar{2}$0) in Ba_2P than in Ba_2As and thus a larger ΔE_{dipole}. We have seen that Ba_2P still has a lower work function than Ba_2As, even though Ba_2As should have a higher E_f on account of its larger d_1. For comparison, the work functions of Ca_2N, Sr_2N, and Ba_2N were also calculated. The results are shown in Figure 6c, where the above argument clearly applies to also explain the observed trend.

Finally, dynamic stability against ion vibration and thermal stability against temperature (e.g., room temperature) were carefully checked for the above three structures. Figure 7a,d,h presents their phonon spectra calculated by the finite displacement method as implemented in Phonopy code.[39] They all have positive phonon frequencies in the whole Brillouin zone, which denotes that the structures are stable with respect to ion vibration modes. In addition, first-principles molecular dynamics (MD) simulations[26] were performed at temperature 350 K using NVT ensemble and Nose–Hoover thermostat. The MD time step was 2 fs, the total simulation

DOI: 10.1021/jacs.6b05586
J. Am. Chem. Soc. 2016, 138, 15336–15344

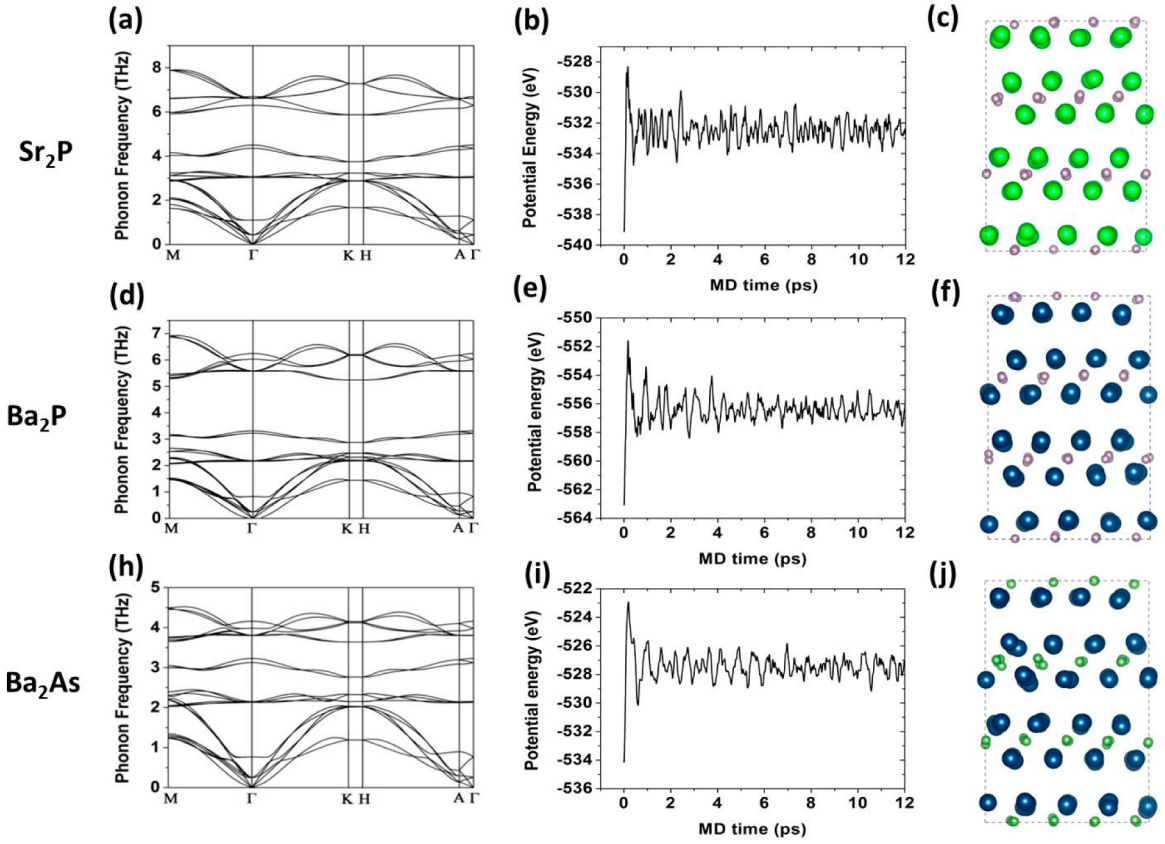

Figure 7. Dynamic and thermal stabilities: (a, d, h) phonon spectrum; (b, e, (i) total potential energy as a function of MD time at temperature of 350 K; (c, f, j) structure snapshots after equilibration.

time was 12 ps, and the simulation cell size contained 144 atoms. We monitored the time evolution of potential energies during the MD simulations as presented in Figure 7b,e,i). The potential energy value reached equilibrium very quickly (in 4 ps) and fluctuated near the equilibrium value. The structure snapshots in Figure 7c,f,j confirm that no destruction of structure occurred in any Sr_2P, Ba_2P, or Ba_2As. We performed MD simulations at higher temperature 700 K, which was an operating temperature for a catalysis application (ammonia synthesis) of another electride, $C_{12}A_7$ loaded with Ru metal, in previous studies.[8−11] We found a little more structural distortion than in 350 K structures, and the potential energy showed larger fluctuations (see Supporting Information Figure S10). However, no structural destruction was observed. We thus conclude that the newly discovered 2D electrides Sr_2P, Ba_2P, and Ba_2As can be stable at temperatures as high as 700 K and that they are interesting candidates for room temperature electride applications as well as high temperature catalysis applications.

We also explored the possibility of 2D electrides using AB composition, with cations remaining to be alkaline-earth elements and anions being halogens (VIIA). Our search results are summarized in the right-most panel of Table 1. Only AF (A = Ca, Sr, Ba) has a layered structure that can support electrides. These three layered electrides all have a tetragonal crystal structure with space group *P*4/*nmm* (#129) in Figure 8a (for more details on structure, including lattice constants and atom positions, see Supporting Information Tables S1 and S3). Their stacking configurations are different from the ionic layer stacking of Ca−N−Ca in Ca_2N, where two Ca atoms sandwich

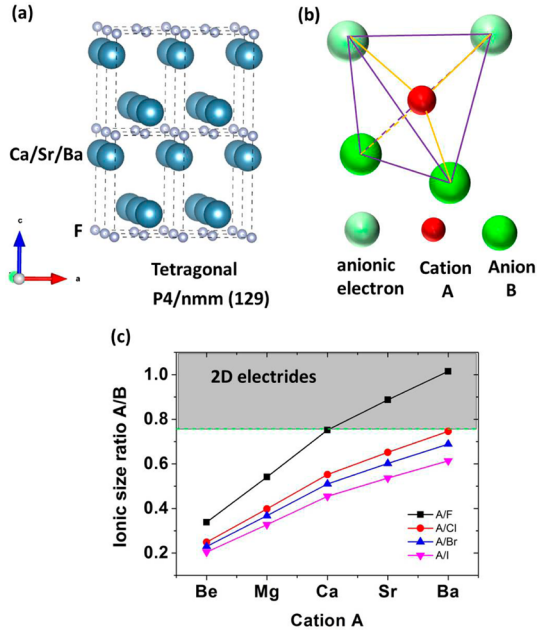

Figure 8. (a) Predicted layered crystal structure for 2D electrides AF (A = Ca, Sr, Ba) with tetragonal crystal and space group space group *P*4/*nmm* (#129). (b) Schematic of cation A centered tetrahedron formed by anion B and anionic electron. (c) Ionic size ratio of A to B as a function of different cation A. The dark gray shaded area denotes the chemical region of AB having electride-supporting layered structure.

DOI: 10.1021/jacs.6b05586
J. Am. Chem. Soc. 2016, 138, 15336−15344

one N atom; AF has A−2F−A stacking, where two A's sandwich two F's (2F) sitting in the same plane. The new stacking fits well with our proposed model of 2D electride structure in Figure 1b2, where a small sized anion is assumed. Because a similar structure is not found when B is replaced by the larger Cl, Br, and I anions, we postulate cation/anion size ratio should again be the critical factor in determining if such a layered structure is preferred. The polyhedrons present in the AF structure are A_4F tetrahedron and also cation A centered tetrahedron formed by anion B and anionic electron at the corners, as depicted in Figure 8b. This cation A centered tetrahedron can be derived by noticing the high distribution of anionic electron density at the cavity of the cation tetrahedron formed by the cations at interlayer space from the adjacent cation layers (see Supporting Information Figure S11−S13). As in layered A_2B above, the stabilization of such a tetrahedron should again be related to sufficiently large cation/anion size ratio, so we therefore plotted it in Figure 8c. The dark gray shaded area, which has a larger size ratio than the rest, contains exactly the same three AF's (A = Ca, Sr, Ba) predicted from our calculations.

The formation energy of AF is positive at ∼0.05−0.09 eV/atom (see Table S3) with respect to the naturally existing stable compound A_2F and the elementary metal A, indicating the predicted AF structure is not thermodynamically stable. On the other hand, our phonon spectrum calculations show that no imaginary frequencies appear in AF (Figure S15) and thus it can be metastable. Our band structure calculations show that AF has very dispersive bands around the Fermi energy, and charge density calculations exhibit a substantial charge distribution in the interlayer space of AF, suggesting it could be 2D electrides (see Supporting Information Figures S11−S14).

Interestingly, experimentally existing layered PbFCl-type compounds AFX (A = Ca, Sr, Ba, Pb, Eu; X = Cl, Br, I)[40,41] have almost the same structure as our predicated AF structure, except that AFX has an X layer in-between two A layers. Conversely, the interlayer space in AF could be viewed to correspond to the region occupied by the X layer in AFX. Besides, experimentally layered stable Ba_2PCl[42] can be mapped to the predicated electride Ba_2P in the same way. This structure correspondence picture turns out to have appeared in electrides $Ca_{24}Al_{28}O_{64}$, Ca_2N, and $La_8Sr_2(SiO_4)_6$ as mentioned in the Introduction. This seemingly indicates a new direction in searching for new 2D electrides based on layered ionic compounds.

CONCLUSIONS

To summarize, we have applied the global structure optimization method together with DFT calculations for total energy, phonon spectrum, and molecular dynamic simulations to predict thermodynamically stable new 2D electrides from A_2B (A/B = alkaline-earth metals/VA, VIA nonmetals) and AB (A/B = alkaline-earth metals/halogen). We have identified layered Sr_2P, Ba_2P, and Ba_2As and CaF, SrF, and BaF as new electrides with interlayer space sandwiched between cation layers, and have further confirmed that they are electride through band structure, charge density, and work function calculations. Most importantly, we have associated the presence of a sandwiched layered structure with the cation/anion size ratio, which has to be large enough to favor the two dimensionality and thereby 2D electride. Our work may open up a new avenue to the discovery of new 2D electrides by global structure search and provide new insight into the principles of electride design.

ASSOCIATED CONTENT

Supporting Information

The Supporting Information is available free of charge on the ACS Publications website at DOI: 10.1021/jacs.6b05586.

Structure information on predicted 2D electrides and ionic sizes in calculating cation/anion size ratio; electron localization function calculations; an atomistic structure of Ca_2O ground state crystal; details of work function calculations; 700 K molecular dynamics simulation of Sr_2P, Ba_2P and Ba_2As; structure information and formation energies of AF (A = Ca, Sr, Ba), their band structures and anionic electron charge density distribution, anionic electron ratio, and phonon spectra (PDF)

AUTHOR INFORMATION

Corresponding Authors

*M. Yoon. Email: myoon@ornl.gov

*S. W. Kim. Email: kimsungwng@skku.edu

Notes

The authors declare no competing financial interest.

ACKNOWLEDGMENTS

Research (W.M. and M.Y.) was performed at the Center for Nanophase Materials Sciences, which is a DOE Office of Science User Facility. This research was supported by Creative Materials Discovery Program through the National Research Foundation of Korea (NRF) funded by the Ministry of Science, ICT and Future Planning (2015M3D1A1070639). W.M. was partly supported by the Laboratory Directed Research and Development Program of Oak Ridge National Laboratory, managed by UT-Battle, LLC, for the U.S. DOE. M.-H.D. was supported by the U.S. Department of Energy, Office of Science, Basic Energy Sciences, Materials Sciences and Engineering Division. Computing resources were provided by the National Energy Research Scientific Computing Center, which is supported by the Office of Science of the U.S. Department of Energy under Contract No. DE-AC02-05CH11231.

REFERENCES

(1) Dye, J. L. *Science* **1990**, *247*, 663.

(2) Singh, D. J.; Krakauer, H.; Haas, C.; Pickett, W. E. *Nature* **1993**, *365*, 39.

(3) Matsuishi, S.; Toda, Y.; Miyakawa, M.; Hayashi, K.; Kamiya, T.; Hirano, M.; Tanaka, I.; Hosono, H. *Science* **2003**, *301*, 626.

(4) Toda, Y.; Yanagi, H.; Ikenaga, E.; Kim, J. J.; Kobata, M.; Ueda, S.; Kamiya, T.; Hirano, M.; Kobayashi, K.; Hosono, H. *Adv. Mater.* **2007**, *19*, 3564.

(5) Toda, Y.; Kim, S. W.; Hayashi, K.; Hirano, M.; Kamiya, T.; Hosono, H.; Haraguchi, T.; Yasuda, H. *Appl. Phys. Lett.* **2005**, *87*, 254103.

(6) Kim, K. B.; Kikuchi, M.; Miyakawa, M.; Yanagi, H.; Kamiya, T.; Hirano, M.; Hosono, H. *J. Phys. Chem. C* **2007**, *111*, 8403.

(7) Yanagi, H.; Kim, K. B.; Koizumi, I.; Kikuchi, M.; Hiramatsu, H.; Miyakawa, M.; Kamiya, T.; Hirano, M.; Hosono, H. *J. Phys. Chem. C* **2009**, *113*, 18379.

(8) Kitano, M.; Inoue, Y.; Yamazaki, Y.; Hayashi, F.; Kanbara, S.; Matsuishi, S.; Yokoyama, T.; Kim, S. W.; Hara, M.; Hosono, H. *Nat. Chem.* **2012**, *4*, 934.

(9) Toda, Y.; Hirayama, H.; Kuganathan, N.; Torrisi, A.; Sushko, P. V.; Hosono, H. *Nat. Commun.* **2013**, *4*, 2378.

DOI: 10.1021/jacs.6b05586
J. Am. Chem. Soc. 2016, 138, 15336−15344

(10) Kitano, M.; Kanbara, S.; Inoue, Y.; Kuganathan, N.; Sushko, P. V.; Yokoyama, T.; Hara, M.; Hosono, H. *Nat. Commun.* **2015**, *6*, 6731.
(11) Sharif, M. J.; Kitano, M.; Inoue, Y.; Niwa, Y.; Abe, H.; Yokoyama, T.; Hara, M.; Hosono, H. *J. Phys. Chem. C* **2015**, *119*, 11725.
(12) Dye, J. L. *Acc. Chem. Res.* **2009**, *42*, 1564.
(13) Dye, J. L. *Science* **2003**, *301*, 607.
(14) Lee, K.; Kim, S. W.; Toda, Y.; Matsuishi, S.; Hosono, H. *Nature* **2013**, *494*, 336.
(15) Li, Z. Y.; Yang, J. L.; Hou, J. G.; Zhu, Q. S. *Angew. Chem., Int. Ed.* **2004**, *43*, 6479.
(16) Zhao, S. T.; Li, Z. Y.; Yang, J. L. *J. Am. Chem. Soc.* **2014**, *136*, 13313.
(17) Reckeweg, O.; DiSalvo, F. J. *Solid State Sci.* **2002**, *4*, 575.
(18) Vajenine, G. V.; Grzechnik, A.; Syassen, K.; Loa, I.; Hanfland, M.; Simon, A. *C. R. Chim.* **2005**, *8*, 1897.
(19) Zhang, Y. Q.; Xiao, Z. W.; Kamiya, T.; Hosono, H. *J. Phys. Chem. Lett.* **2015**, *6*, 4966.
(20) Markham, J. J. *F-Centers in Alkali Halides*; Academic Press: New York, 1966.
(21) Tada, T.; Takemoto, S.; Matsuishi, S.; Hosono, H. *Inorg. Chem.* **2014**, *53*, 10347.
(22) Inoshita, T.; Jeong, S.; Hamada, N.; Hosono, H. *Phys. Rev. X* **2014**, *4*, 031023.
(23) Zhang, Y. W. H.; Wang, Y.; Zhang, L.; Ma, Y. *arXiv*:1603.04161.
(24) Wang, Y. C.; Lv, J. A.; Zhu, L.; Ma, Y. M. *Phys. Rev. B: Condens. Matter Mater. Phys.* **2010**, *82*, 094116.
(25) Wang, Y. C.; Lv, J.; Zhu, L.; Ma, Y. M. *Comput. Phys. Commun.* **2012**, *183*, 2063.
(26) Kresse, G.; Furthmuller, J. *Comput. Mater. Sci.* **1996**, *6*, 15.
(27) Kresse, G.; Joubert, D. *Phys. Rev. B: Condens. Matter Mater. Phys.* **1999**, *59*, 1758.
(28) Perdew, J. P.; Burke, K.; Ernzerhof, M. *Phys. Rev. Lett.* **1996**, *77*, 3865.
(29) Zhang, X.; Xiao, Z. W.; Lei, H. C.; Toda, Y.; Matsuishi, S.; Kamiya, T.; Ueda, S.; Hosono, H. *Chem. Mater.* **2014**, *26*, 6638.
(30) Sushko, P. V.; Shluger, A. L.; Hayashi, K.; Hirano, M.; Hosono, H. *Phys. Rev. B: Condens. Matter Mater. Phys.* **2006**, *73*, 045120.
(31) Walsh, A.; Scanlon, D. O. *J. Mater. Chem. C* **2013**, *1*, 3525.
(32) Dale, S. G.; Otero-de-la-Roza, A.; Johnson, E. R. *Phys. Chem. Chem. Phys.* **2014**, *16*, 14584.
(33) Pauling, L. *J. Am. Chem. Soc.* **1929**, *51*, 1010.
(34) Hakkinen, H.; Barnett, R. N.; Landman, U. *Chem. Phys. Lett.* **1995**, *232*, 79.
(35) Hakkinen, H.; Barnett, R. N.; Landman, U. *Europhys. Lett.* **1994**, *28*, 263.
(36) Jain, A.; Ong, S. P.; Hautier, G.; Chen, W.; Richards, W. D.; Dacek, S.; Cholia, S.; Gunter, D.; Skinner, D.; Ceder, G.; Persson, K. A. *APL Mater.* **2013**, *1*, 011002.
(37) Smoluchowski, R. *Phys. Rev.* **1941**, *60*, 661.
(38) Methfessel, M.; Hennig, D.; Scheffler, M. *Phys. Rev. B: Condens. Matter Mater. Phys.* **1992**, *46*, 4816.
(39) Togo, A.; Oba, F.; Tanaka, I. *Phys. Rev. B: Condens. Matter Mater. Phys.* **2008**, *78*, DOI: 10.1103/PhysRevB.78.134106.
(40) Decremps, F.; Fischer, M.; Polian, A.; Itie, J. P.; Sieskind, M. *Phys. Rev. B: Condens. Matter Mater. Phys.* **1999**, *59*, 4011.
(41) Shen, Y. R.; Englisch, U.; Chudinovskikh, L.; Porsch, F.; Haberkorn, R.; Beck, H. P.; Holzapfel, W. B. *J. Phys.: Condens. Matter* **1994**, *6*, 3197.
(42) Materials Project structure data Ba_2PCl. https://www.materialsproject.org/materials/mp-27869.

DOI: 10.1021/jacs.6b05586
J. Am. Chem. Soc. 2016, 138, 15336−15344